Structural Engineering and Mechanics, Vol. 45, No. 5 (2013) 613-629

DOI: http://dx.doi.org/10.12989/sem.2013.45.5.613

Out-of-plane elastic buckling of truss beams

Alexis Fedoroff*[1] and Reijo Kouhia[2]

[1]Department of Civil and Structural Engineering, Aalto University, Rakentajanaukio 4 A, Otaniemi, Espoo, Finland
[2]Department of Engineering Design, Tampere University of Technology, Korkeakoulunkatu 10, 33720 Tampere, Finland

(Received July 6, 2011, Revised January 12, 2013, Accepted February 19, 2013)

Abstract. In this article we will present a method to directly evaluate the critical point of a non-linear system by using the solution of a polynomial eigenvalue approximation as a starting point for an iterative non-linear system solver. This method will be used to evaluate out-of-plane buckling properties of truss structures for which the lateral displacement of the upper chord has been prevented. The aim is to assess for a number of example structures whether or not the linearized eigenvalue solution gives a relevant starting point for an iterative non-linear system solver in order to find the minimum positive critical load.

Keywords: truss structures; out-of-plane buckling; non-linear iterative solver; polynomial eigenvalue problem

1. Introduction

In civil engineering and building construction the truss is, indeed, a widely used structural element. As soon as the span is long enough, the only practical choice left to support the roof of an industrial building or sports hall is a steel truss. More recently long-span wood trusses have become popular in wooden construction, too, and even in lightweight building structures trusses made up from cold formed profiles have made their breakthrough. In the situations that have just been exposed the advantages of a steel truss over a hot rolled or welded profile are obvious. For equal load carrying capacity a truss provides a much lighter structure than rolled or welded profile, and additionally the open spaces between the diagonals of a truss can be naturally used to support ducts or other mechanical equipment. Finally, if we think of the construction time logistics, the truss alternative provides more flexibility: it is fairly easy to design a long-span truss made up of partial assemblies that are manufactured and delivered on site independently.

After having set forth the advantages of a truss structure over a beam made of a solid cross-section (i.e., a hot rolled or welded structure), let's examine some of the drawbacks, or rather some problems related to the analysis of truss structures. As a rule of thumb, bulky structures are stable by nature whereas slender structures are prone to geometric instabilities. Let's qualitatively compare the geometric instabilities which may occur for various types of cross-sections of a flexurally loaded beam. If we first consider a rectangular solid cross-section, the beam can be

*Corresponding author, Ph.D. Student, E-mail: alexis.fedoroff@aalto.fi

loaded until material failure without any geometric instability. Now if we consider a thin-walled profile[1], depending on the dimensions and loading, we can potentially observe lateral buckling, cross-sectional distortional buckling, and local plate buckling, or any combination thereof. All of these buckling phenomena have been widely studied by Vlasov (1961), who set up the global buckling theory for thin-walled beams. Later, distortional buckling has been studied by Sridharan and Rafael (1985), Hancock *et al.* (1990), Vrcelj and Bradford (2006), and in general local-global buckling interaction has been the object of a large number of studies. Now if we come back to our main subject of interest, the truss beam, we can only imagine the number of possibilities for geometric instabilities if we assume that each member of the truss structure is a thin-walled beam with axial and flexural loading. Consequently any member of the truss can buckle flexurally, torsionally or laterally in a memberwise global way, and additionally each member can exhibit distortional or local buckling. However, memberwise buckling is not all we have. Assuming that the nodal points of the truss are free to move out of the plane in which they were initially set, we can possibly observe "rigid body rotation" of the truss members, in addition to memberwise buckling. This out-of-plane rigid body motion can be viewed as some sort of lateral buckling of the entire truss frame.

As we can see, the range of geometric instability phenomena in an assumed perfectly elastic structure is very large. In addition, any given buckling mode of a truss structure is typically a combination of those "elementary buckling modes". Attempts to systematically classify instability phenomena related to frame and truss structures[2] have been made in Trahair (1975), Trahair and Chan (2003). Even if it has been clear from the early days that plane trusses are prone to global out-of-plane instabilities (Masur and Cukurs 1956), most of the recent studies are concentrated on memberwise out-of-plane buckling with nodal lateral displacement explicitly restricted (Trahair 2009), although Iwicki (2010) considers a truss example with elastic springs in the lateral direction applied at top chord nodes while the lower chord nodes are free to move. In Chan and Cho (2008) an interesting full scale experiment is made with a Warren truss, and although nodal lateral displacement is not restricted, the buckling mode is clearly of memberwise out-of-plane type.

Real buckling behavior is often so complex, that it makes sense to discard by assumption some of the elementary buckling possibilities based on physical and engineering considerations. Therefore we shall assume in our kinematical model that for instance local and distortional buckling is prevented, which simplifies our modeling task. The kinematics and the resulting system of differential equation that modelizes the behavior of a given member of the truss structure are the ones first introduced in Vlasov (1961), commonly referred to as the "buckling equations" or "second order theory equations". Although more developed beam theories are available since then (Schardt 1966, Attard 1990), traditional beam theory has been estimated accurate enough, at least as a first approach, to analyze buckling phenomena in trusses. Since we assume that external forces apply only on nodal points and the displacements and rotations at the nodal points are by definition the system's state variables, the mathematical model of a given member can be seen as a boundary control system modeled by a homogeneous ODE. If we substitute the boundary controlled solution of this ODE in the continuous formulations of the

---

[1]The cross-sectional normal dimension (wall thickness) is small compared to the tangential dimension (width/height of the beam)

[2]Traditionally a truss is a structure with moment free connection and a frame is a structure with moment rigid connections. In this article we consider all connections to be moment rigid unless otherwise specified. Hence a truss and a frame can be viewed as synonyms.

equilibrium and criticality conditions, we get as a result a discrete non-linear formulation. The discrete non-linear formulation of the equilibrium and criticality conditions for the whole truss is then just the assembly of the memberwise discrete formulations. This rather unorthodox way to implement a discretization is just a finite element method where the test functions fulfill the homogeneous differential equations pointwise.

Usually engineers designing long-span truss beams are well aware of the lateral buckling risk in case the upper chord of the beam is free to move sideways. Non-linear analysis is then performed using finite element model together with some sort of numerical tool to find the critical point. This could be either a path following method or it could be a method based on the linearization (with respect to the load parameter) of the non-linear eigenvalue problem. However, this kind of situations where non-trivial computation is needed are usually avoided by designers, which prefer to use structural solutions that are inherently stable for example by applying bracing to avoid lateral movement of the upper chord. Besides, this kind of situation arises often naturally if we consider that purlins and roof sheeting provide sufficient stiffness to oppose to any lateral movement of the upper chord of the truss beam. Then, by analogy with the Vlasov theory applied to thin-walled solid cross-section beams, one can argue that the lateral buckling load of a thin-walled beam with upper chord lateral movement restricted is infinitely high. Using that result, one can say that if the structure does not buckle as a whole, then the only thing that needs to be checked is the memberwise buckling of each member. However, as we will soon show in this article, the analogy between lateral buckling of truss beams and lateral buckling of solid cross-section beams does not, unfortunately, hold. Indeed, we will show examples of trusses where we can observe, in addition to memberwise buckling, "rigid body rotation" of the diagonals, even when the lateral movement of the upper chord is restricted.

The existence of this given buckling mode is one part of the problem. Of course we must asses whether it occurs within the elastic bounds of the material, and if it does, whether the post-buckling path in the neighborhood of the critical point is stable or unstable. But, in addition to that, we must be able to compute numerically the critical point and eventually, by using numerical Lyapunov-Schmidt reduction (Govaerts 2000), the post-buckling stability assessment. We already stated two numerical tools to find the critical point, namely the path following method and the linearization method. The first one has proven to be robust, but since we have to compute a number of equilibrium points, it is often time consuming and requires interaction from the operator in the choice of parameters such as the arc-length step. The second method is usually more expeditive. The criticality condition can be viewed as a non-linear eigenvalue problem and can therefore be approximated by a linearization with respect to the load parameter and evaluated at the origin. Probably simplicity of this method, both in use and implementation, has made it so popular in commercial finite element packages. However, here, too, some caveats have to be taken into consideration. First, if the system behavior is highly non-linear in the pre-critical state, then obviously the linearized eigenvalue problem will lead to a very bad approximation. This is actually what is happening with the truss beam with restricted upper chord lateral motion. One can easily intuitively feel that if we compare two identical trusses, one with non-restricted upper chord lateral motion and a second one with restricted upper chord lateral motion, the critical load in the second case must be much higher due to higher stiffness of the system. Therefore the pre-critical path in the second case will extend much further in the non-linear domain, which leads to bad approximations if we use linearized eigenvalue problem. A remedy will be proposed, and it is the quadratic (or higher order polynomial) approximation of the eigenvalue problem. One can even imagine a more radical case: what if the first order coefficient matrix vanishes altogether or degenerates in such a way that the result is physically meaningless?

Now we shall expose more in details some of the ideas given in this introduction. First, section 2 will be devoted to the main issues of the mathematical model, which will be used as a basis for subsequent stability analyses. Then, in section 3, a procedure for direct computation of the critical point will be set up and finally critical properties of some example trusses will be analyzed in section 4.

2. The mathematical model

We would like to set up here a mathematical model that enables us to perform a stability analysis of a given truss structure, assumedly geometrically perfect. As we already stated in the introductory part, the study will focus on plane trusses with out-of-plane buckling modes. An example of such a truss is given in Fig. 1.

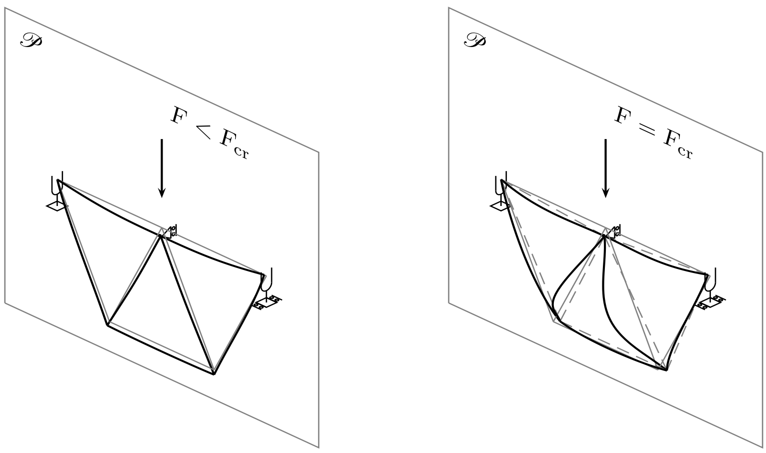

Fig. 1 Initially plane truss with in-plane primary path and out-of-plane buckling mode

Consider intuitively what could happen if we start loading this example truss with a load that lies in the plane $\mathscr{P}$. When we start loading the truss in a quasi-static way, the truss will deform, but the deformed shape will still stay within the initial plane $\mathscr{P}$. This in-plane state of deformation, which lasts up to the critical point, will be referred to as the primary state. We will assume that neither limit points (i.e., snap through) nor bifurcations (i.e., in-plane buckling) will occur in the primary state, which enables us to concentrate on the out-of-plane buckling behaviour. When the critical load is reached, the primary state is no longer stable and hence the system bifurcates to the secondary state of equilibrium, which is characterized by out-of-plane displacements of some of the members and/or nodes of the truss. Analysis of the post-buckling behaviour in the neighbourhood of the critical point requires a mathematical technique called the Lyapunov-Schmidt reduction (Koiter 1945, Golubitsky and Schaeffer 1985), but in order to analyze the post-buckling behaviour we need first to compute the critical point and the buckling mode, so we shall concentrate on that aspect first.

Now let's find out how to define the state variables of our system in such a way that we have a minimal amount of them. The answer is of course that we should have one element per member, i.e. twelve degrees of freedom per member (three displacement d.o.f. plus three rotational d.o.f. at each end). Implementation is done by choosing test functions in such a way that they pointwise fulfil the homogeneous differential equations given by the strong form of the equilibrium and criticality conditions. The state variables are then defined as the Dirichlet boundary conditions to the given differential equations. A remark can be made on the definition of stability used in our approach. We will use the energy criterion for stability and assume that it is, for all practical purposes, equivalent to the Lyapunov (dynamic) criterion for stability. The equivalence theorem has been proven in (Koiter 1945). Criticality criterion (i.e., Trefftz condition) is then just defined as the boundary between stable and unstable domains.

The truss system we are about to investigate for equilibrium and criticality consists of a finite number of members and nodes. Each member is modeled using any of the available beam theories: Euler-Bernoulli or Timoshenko beam theory for prismatic cross-sections, Vlasov beam theory for open or closed thin-walled cross-sections, or any other second order theory, provided we are able to solve it analytically. Consider a very general way of noting the equilibrium in primary state (1a) and criticality (1b) differential equations. The equilibrium in primary state and criticality conditions can be given as a boundary controlled Dirichlet problem where the homogeneous ODE linear operator $\mathscr{L}\,|_{\hat{\mathbf{u}}_\mathrm{I}}$ depends on the boundary control value $\hat{\mathbf{u}}_\mathrm{I}$ and in general the linear operator is not constant. (The ODE may be assumed homogeneous since we consider external loads to be applied only on truss nodes.)

$$\begin{cases} \mathscr{L}\,|_{\hat{\mathbf{u}}_\mathrm{I}}\ \mathbf{u}_\mathrm{I} = 0 & \text{inside the domain } \Omega \\ \mathbf{u}_\mathrm{I} = \hat{\mathbf{u}}_\mathrm{I} & \text{on the boundary } \partial\Omega \end{cases} \tag{1a}$$

$$\begin{cases} \mathscr{L}\,|_{\hat{\mathbf{u}}_\mathrm{I}}\ \mathbf{v} = 0 & \text{inside the domain } \Omega \\ \mathbf{v} = \hat{\mathbf{v}} & \text{on the boundary } \partial\Omega \end{cases} \tag{1b}$$

The notation $(\cdot)_\mathrm{I}$ implies that the vector or vector valued function is restricted to the subset of $\mathbb{R}^6$ such as all out-of-plane displacements and rotations are zero. If we now consider the internal energy contribution to the equilibrium condition $\delta U\,|_{\mathbf{u}_\mathrm{I}}\,(\mathbf{v}_\mathrm{I})$ (i.e. the variation of the internal energy in the direction $\mathbf{v}_\mathrm{I}$ evaluated at $\mathbf{u}_\mathrm{I}$) and the internal energy contribution to the criticality condition $\delta\left(\tfrac{1}{2}\,\delta^2 U\,|_{\mathbf{u}_\mathrm{I}}\right)|_{\mathbf{v}}\,(\mathbf{w})$ (i.e. the variation of the second variation of the internal energy in the direction $\mathbf{w}$ evaluated at $\mathbf{v}$), we may say that both those objects are bilinear symmetric functionals that depend on the boundary control value $\hat{\mathbf{u}}_\mathrm{I}$. Integration by part of these functionals will yield a boundary term and a field term

$$\delta U\,|_{\mathbf{u}_\mathrm{I}}\,(\mathbf{v}_\mathrm{I}) = \begin{pmatrix} \hat{\mathbf{v}}_\mathrm{I}(0) \\ \hat{\mathbf{v}}_\mathrm{I}(1) \end{pmatrix}^\mathsf{T} \begin{pmatrix} \mathbf{K}_{00} & \mathbf{K}_{01} \\ \mathbf{K}_{10} & \mathbf{K}_{11} \end{pmatrix}_{|\hat{\mathbf{u}}_\mathrm{I}} \begin{pmatrix} \hat{\mathbf{u}}_\mathrm{I}(0) \\ \hat{\mathbf{u}}_\mathrm{I}(1) \end{pmatrix} + \int_\Omega \mathbf{v}_\mathrm{I}^{\,\mathsf{T}}\,\mathscr{L}\,|_{\hat{\mathbf{u}}_\mathrm{I}}\ \mathbf{u}_\mathrm{I} \tag{2a}$$

$$\delta\left(\tfrac{1}{2}\,\delta^2 U\,|_{\mathbf{u}_\mathrm{I}}\right)|_{\mathbf{v}}\,(\mathbf{w}) = \begin{pmatrix} \hat{\mathbf{w}}(0) \\ \hat{\mathbf{w}}(1) \end{pmatrix}^\mathsf{T} \begin{pmatrix} \mathbf{K}_{00} & \mathbf{K}_{01} \\ \mathbf{K}_{10} & \mathbf{K}_{11} \end{pmatrix}_{|\hat{\mathbf{u}}_\mathrm{I}} \begin{pmatrix} \hat{\mathbf{v}}(0) \\ \hat{\mathbf{v}}(1) \end{pmatrix} + \int_\Omega \mathbf{w}^\mathsf{T}\,\mathscr{L}\,|_{\hat{\mathbf{u}}_\mathrm{I}}\ \mathbf{v} \tag{2b}$$

The field term vanishes due to the relations (1a) and (1b). From now on, let's explicitly mention the elementwise character of any given quantity by apposing the superscript $(\cdot)^{(e)}$. If we introduce the following new notation for the boundary control terms $\mathbf{p}^{(e)}$, $\mathbf{q}^{(e)}$ and $\mathbf{r}^{(e)} \in \mathbb{R}^{12}$ which take entries of the vectors $\left(\hat{\mathbf{u}}(0)^{\mathsf{T}} \quad \hat{\mathbf{u}}(1)^{\mathsf{T}}\right)^{\mathsf{T}}$, $\left(\hat{\mathbf{v}}(0)^{\mathsf{T}} \quad \hat{\mathbf{v}}(1)^{\mathsf{T}}\right)^{\mathsf{T}}$ and $\left(\hat{\mathbf{w}}(0)^{\mathsf{T}} \quad \hat{\mathbf{w}}(1)^{\mathsf{T}}\right)^{\mathsf{T}}$ and rearrange them appropriately, we end up with the following elementwise notation

$$\delta U^{(e)}\,|_{\mathbf{u}_{\mathrm{I}}}\,(\mathbf{v}_{\mathrm{I}}) = \mathbf{q}_{\mathrm{I}}^{(e)^{\mathsf{T}}}\mathbf{K}_{\mathrm{I}}^{(e)}\,|_{\mathbf{p}_{\mathrm{I}}^{(e)}}\,\mathbf{p}_{\mathrm{I}}^{(e)} \tag{3a}$$

$$\delta\left(\tfrac{1}{2}\,\delta^2 U^{(e)}\,|_{\mathbf{u}_{\mathrm{I}}}\right)|_{\mathbf{v}}\,(\mathbf{w}) = \begin{pmatrix}\mathbf{r}_{\mathrm{I}}^{(e)}\\ \mathbf{r}_{\mathrm{II}}^{(e)}\end{pmatrix}^{\mathsf{T}}\begin{pmatrix}\mathbf{K}_{\mathrm{I}}^{(e)} & 0\\ 0 & \mathbf{K}_{\mathrm{II}}^{(e)}\end{pmatrix}_{|\mathbf{p}_{\mathrm{I}}^{(e)}}\begin{pmatrix}\mathbf{q}_{\mathrm{I}}^{(e)}\\ \mathbf{q}_{\mathrm{II}}^{(e)}\end{pmatrix} \tag{3b}$$

Note that the block diagonal form of the non-linear stiffness matrix in the criticality condition is a direct consequence of the fact that in the strong form of the criticality condition (1b), which has to be viewed as a system of ODE, the equation lines related to the primary state variables are uncoupled with respect to the equation lines related to secondary state variables. Considering the transform matrix $\boldsymbol{\alpha}^{(e)}$ which maps the global state vector $\mathbf{p}$ to the elementwise local state vector $\mathbf{p}^{(e)}$ and taking the sum over all elements we can express the internal energy contribution of the full system to the equilibrium and criticality conditions, where the global stiffness matrices are given by the relations $\mathbf{K}_{\mathrm{I}} = \sum_e \boldsymbol{\alpha}_{\mathrm{I}}^{(e)^{\mathsf{T}}}\mathbf{K}_{\mathrm{I}}^{(e)}\boldsymbol{\alpha}_{\mathrm{I}}^{(e)}$ and $\mathbf{K}_{\mathrm{II}} = \sum_e \boldsymbol{\alpha}_{\mathrm{II}}^{(e)^{\mathsf{T}}}\mathbf{K}_{\mathrm{II}}^{(e)}\boldsymbol{\alpha}_{\mathrm{II}}^{(e)}$. We can therefore assess the equivalence between the continuous formulations of equilibrium and criticality conditions

$$\begin{cases}\delta U\,|_{\mathbf{u}_{\mathrm{I}}}\,(\mathbf{v}_{\mathrm{I}}) & = & \delta V\,|_{\mathbf{u}_{\mathrm{I}}}\,(\mathbf{v}_{\mathrm{I}}) & \forall \mathbf{v}_{\mathrm{I}} \in \mathscr{V}_{\mathbf{u}_{\mathrm{I}}}\\ \delta\left(\tfrac{1}{2}\,\delta^2 U\,|_{\mathbf{u}_{\mathrm{I}}}\right)|_{\mathbf{v}}\,(\mathbf{w}) & = & 0 & \forall \mathbf{w} \in \mathscr{V}_{\mathbf{v}}\end{cases} \tag{4a}$$

$$\begin{cases}\mathbf{q}_{\mathrm{I}}^{\mathsf{T}}\mathbf{K}_{\mathrm{I}}\,|_{\mathbf{p}_{\mathrm{I}}}\,\mathbf{p}_{\mathrm{I}} & = & \lambda\,\mathbf{q}_{\mathrm{I}}^{\mathsf{T}}\mathbf{e}_{\mathrm{I}} & \forall \mathbf{q}_{\mathrm{I}} \in \mathscr{V}_{\mathbf{p}_{\mathrm{I}}}\\ \begin{pmatrix}\mathbf{r}_{\mathrm{I}}\\ \mathbf{r}_{\mathrm{II}}\end{pmatrix}^{\mathsf{T}}\begin{pmatrix}\mathbf{K}_{\mathrm{I}} & 0\\ 0 & \mathbf{K}_{\mathrm{II}}\end{pmatrix}_{|\mathbf{p}_{\mathrm{I}}}\begin{pmatrix}\mathbf{q}_{\mathrm{I}}\\ \mathbf{q}_{\mathrm{II}}\end{pmatrix} & = & 0 & \forall \mathbf{r} \in \mathscr{V}_{\mathbf{q}}\end{cases} \tag{4b}$$

Equivalence between the relations (4a) and (4b) can be seen as the main result of section 2. If we solve the discrete non-linear system of equations given by (4b), then we have the exact analytic solution to the continuous non-linear system given by (4a).

3. Numerical evaluation of critical point

Numeric computation of the critical point by indirect methods, which are essentially of path following type, have been object of a large number of publications: Riks (1974), Seydel (1979), Rheinboldt (1986) and more recently Lopez (2002). Those methods are certainly robust, but they are relatively slow to use, need a certain amount of experience from the user and in case we want to run a big number of critical point estimations with parameter variations in the system, indirect methods don't seem to be the easiest way to implement an automated procedure. Instead, direct computation methods to find the critical point would are more appropriate. By direct computation of the critical point we mean here an iterative method which converges to the critical point as opposed to an indirect method, which merely gives upper and lower bounds, such that the determinant of the defining function jacobian changes sign in between.

A classical way to compute directly the critical point is to solve the augmented system of non-linear equations made up of the equilibrium, criticality and normalization conditions, (Keener and Keller 1973, Moore and Spence 1980, Wriggers and Simo 1990), more recently (Battini *et al.* 2003) and (Mäkinen *et al*. 2011). However, if we start the Newton iteration which solves the augmented non-linear system at the origin (with random initial eigenvector), the chances that the Newton iteration converges to the lowest positive eigenpair (which is the one we are usually interested in) are very slim. A better strategy would be to start from a point which has a better chance to lie in the attraction sphere of the minimum positive eigenpair solution. Polynomial expansion of the non-linear eigenproblem given by the criticality condition yields a good approximation for the starting point of a Newton iteration of the augmented system of non-linear equations, provided that the polynomial expansion is accurate enough. Practically, commercial finite element packages seem to rely on the first order approximation which can be inaccurate if the original system is highly non-linear. In such a case second or higher order approximation endows us, obviously, with a better starting point for iterative computation. However higher order expansion has its cost: first order approximation requires first order derivative of the jacobian, second order approximation requires second order derivative of the jacobian, and so on. For practical reasons only linearized and quadratic eigenproblem approximations will be considered, and as we will show, quadratic approximation will usually show to be sufficient when linearized approximation fails.

In this overview of the theory of numeric evaluation of the critical point we shall first concentrate on an abstract non-linear eigenvalue problem and study polynomial approximation thereof. Subsequently we will show how to formulate a polynomial approximation of a criticality condition related to a given mechanical system.

3.1 Non-linear eigenvalue problem and its polynomial approximation

Consider a general non-linear eigenvalue problem

$$\mathbf{A}\,|_{\lambda}\ \mathbf{q} = \mathbf{0} \tag{5}$$

where $\mathbf{A} \in C^{\infty}(\mathbb{R};\mathbb{R}^{n\times n})$ is a smooth matrix valued function of some parameter and $\mathbf{q} \in \mathbb{R}^{n}$ is the eigenvector corresponding to the given problem. The polynomial approximation to a given order k is thus

$$\mathbf{A}\,|_{\lambda}\ \mathbf{q} = \sum_{i=0}^{k} \frac{\lambda^{i}}{i!} \left.\frac{\mathrm{d}^{i}\,\mathbf{A}}{\mathrm{d}\lambda^{i}}\right|_{\lambda} \mathbf{q} + O(\lambda^{k+1}) \tag{6}$$

For future use, assume the following shorthand notations for the derivatives $\mathrm{d}\cdot/\mathrm{d}\lambda =: (\cdot)'$ and $\mathrm{d}^{2}\cdot/\mathrm{d}\lambda^{2} =: (\cdot)''$. Let's try to visualize the behavior of a non-linear eigenvalue problem in the Euclidean matrix space $\mathbb{R}^{n\times n}$. The set of points in that matrix space for which the matrix is singular of rank $n-1$ can be viewed as a smooth $n^{2}-1$ dimensional manifold. Formally define it as follows: $\mathscr{M}_1 := \{\mathbf{X} \in \mathbb{R}^{n \times n} : \operatorname{rank}(\mathbf{X}) = n-1\}$. If rank deficiency p is higher than 1, then the corresponding manifold $\mathscr{M}_p$ is a submanifold of $\mathscr{M}_1$.On the other hand the set of points in the matrix space $\mathbb{R}^{n \times n}$ that correspond to the image of the matrix valued function $\mathbf{A}$ is obviously a one dimensional smooth manifold, note it $\mathscr{I}$. The possible intersection points of $\mathscr{I}$ with $\mathscr{M}_1$ then gives the (real) solutions of the eigenvalue problem $\mathbf{A}|_\lambda \mathbf{q} = \mathbf{0}$. No intersection means the solutions are complex.

Consider now the visualization of a polynomial expansion of our given eigenvalue problem. One can guess that a linear approximation (evaluated, for instance at the origin) is expressed by a straight tangent line to the manifold $\mathscr{I}$ at that given point, whereas the quadratic approximation yields some kind of curve. On Fig.2 we have pictured an example of a non-linear function with linear approximation on the left picture and quadratic approximation on the right picture. We can clearly observe that if the non-linear function is highly non-linear, as it is the case in the given example, then the result $\lambda^{(0)}$ of the linear approximation $(\mathbf{A}|_0 + \lambda^{(0)}\mathbf{A}'|_0)\mathbf{q} = \mathbf{0}$ is much higher than the minimum positive eigenvalue of the non-linear problem, which is our target.

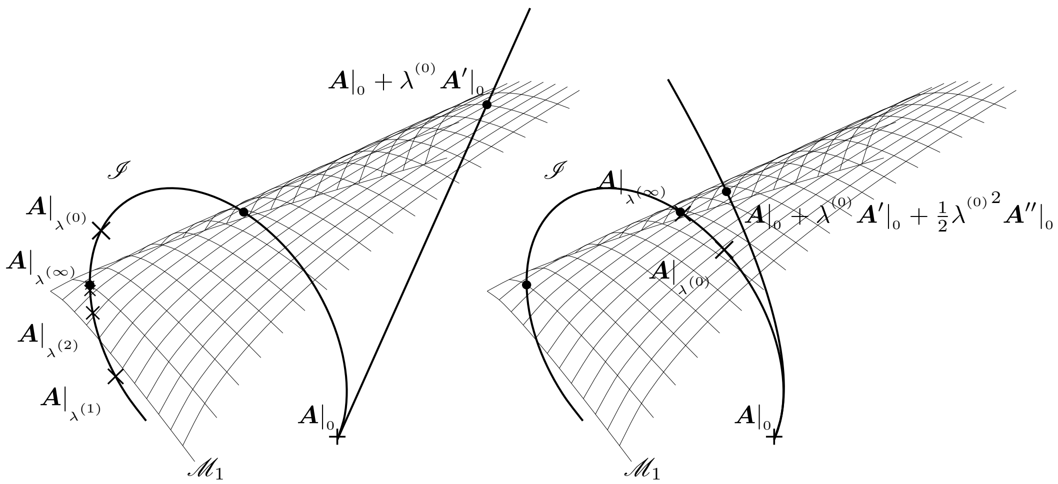

Fig. 2 Example when Newton method fails to converge to the minimum positive eigenvalue if the initial guess is the result of the linearized eigenproblem.

If we take the result of the linear approximation as a starting point to a Newton iteration method to solve the augmented system consisting of the eigenvalue problem and a normalization condition for the eigenvector (Eq. (7)), the solution converges to the second positive eigenvalue of the non-linear problem. This is clearly not what we want.

$$\begin{cases} \mathbf{A}|_\lambda \mathbf{q} & = \mathbf{0} \\ N(\mathbf{q}) & = 0 \end{cases} \tag{7}$$

As a remedy, we recommend the use of quadratic approximation of the non-linear eigenvalue problem $(\mathbf{A}|_0 + \lambda^{(0)}\mathbf{A}'|_0 + \tfrac{1}{2}\lambda^{(0)^2}\mathbf{A}''|_0)\mathbf{q} = \mathbf{0}$ instead of the linear one. On the right picture in Fig. 2, we can see that the result of the quadratic approximation are much closer to the minimum positive solution of the non-linear problem, and if we take the result of the quadratic approximation as a starting point to solve (7) by Newton iteration, then the method converges to the minimum positive solution, which is exactly what we are expecting.

The example given here above is well behaving in the sense that both the linearized and quadratic eigenvalue problems gave real solutions, even though they were not necessarily those we were expecting. However, we can easily imagine cases where especially the linearized eigenvalue problem fails to give real positive results or real results altogether, which can happen if the tangent to the matrix function evaluated at the origin does not intersect the rank deficiency manifold $\mathscr{M}_1$. The most spectacular type of failure is when the first order coefficient matrix is zero, i.e., $\mathbf{A}'|_0 = \mathbf{0}$. Then, obviously the linearized eigenvalue problem does not make sense anymore. In these situations the first order coefficient matrix will be called degenerate.

3.2 Application of polynomial approximation to the criticality condition

Now that we have considered the problematics associated to the polynomial approximation of a non-linear eigenvalue problem, let's briefly formulate the polynomial approximation of criticality condition at equilibrium state evaluated at a given point (which we assume is not critical). Usually the evaluation point is the origin. The procedure is fairly simple. We solve the state vector as a function of the load parameter and substitute it in the criticality condition. Obviously, in a general case solving the equilibrium state analytically is not possible, but we use the implicit function theorem on the equilibrium equation to assume the existence of the state vector as a function of the load parameter in a neighborhood of the evaluation point. The formulation of the polynomial approximation shall first be applied to a general discrete defining function $\mathbf{\Phi} \in \mathcal{C}(\mathbb{R}^{n+1};\mathbb{R}^n)$ and later those results shall be given for the discretized continuous non-linear system, too (as introduced in section 2).

Consider a discrete system, which is mathematically characterized by the function $\mathbf{\Phi}$ defining the equilibrium equation. In subsequent paragraphs we will juts refer to $\mathbf{\Phi}$ as the defining function. At equilibrium and critical point the following set of equations hold

$$\begin{cases} \mathbf{\Phi}(\mathbf{p},\lambda) & = \mathbf{0} \\ \partial_{\mathbf{p}}\mathbf{\Phi}\,|_{(\mathbf{p},\lambda)}\;\mathbf{q} & = \mathbf{0} \end{cases} \tag{8}$$

Assuming that $\partial_{\mathbf{p}}\mathbf{\Phi}\,|_{(\mathbf{0},0)}$ is not singular, by implicit function theorem we have $\mathbf{p} \in \mathcal{C}^\infty(\mathcal{V}_{|\lambda=0};\mathcal{V}_{|\mathbf{p}=\mathbf{0}})$ from an open neighborhood of $\lambda = 0$ to an open neighborhood of $\mathbf{p} = \mathbf{0}$, such as $\mathbf{p}(0) = \mathbf{0}$. Then the polynomial approximation evaluated at the origin with respect to the parameter λ up to the second order term is given as follows (recall the notation $\mathrm{d}\cdot/\mathrm{d}\lambda =: (\cdot)'$).

$$\mathbf{\Phi} + \mathbf{\Phi}'\lambda + ½\mathbf{\Phi}''\lambda^2 + O(\lambda^3) = \mathbf{0} \tag{9a}$$

$$\partial_{\mathbf{p}}\mathbf{\Phi}\,\mathbf{q} + (\partial_{\mathbf{p}}\mathbf{\Phi}\,\mathbf{q})'\lambda + ?\;\;\partial_{\mathbf{p}}\mathbf{\Phi}\,\mathbf{q})''\lambda^2 + O(\lambda^3) = \mathbf{0} \tag{9b}$$

The coefficient expressions of the equilibrium equation (9a) are the following: $\mathbf{\Phi}' = \partial_{\mathbf{p}}\mathbf{\Phi}(\mathbf{p}') + \partial_\lambda\mathbf{\Phi}$ and $\mathbf{\Phi}'' = \partial^2_{\mathbf{p}}\mathbf{\Phi}(\mathbf{p}',\mathbf{p}') + 2\partial_{\mathbf{p}}\partial_\lambda\mathbf{\Phi}(\mathbf{p}') + \partial_{\mathbf{p}}\mathbf{\Phi}(\mathbf{p}'') + \partial^2_\lambda\mathbf{\Phi}$. The coefficient expressions of the criticality condition (9b) are given as follows: $(\partial_{\mathbf{p}}\mathbf{\Phi}\,\mathbf{q})' =$

$(\partial_{\mathbf{p}}^2 \mathbf{\Phi}(\mathbf{p}') + \partial_{\mathbf{p}}\partial_\lambda \mathbf{\Phi})\mathbf{q}$ and $(\partial_{\mathbf{p}}\mathbf{\Phi}\,\mathbf{q})'' = (\partial_{\mathbf{p}}^3 \mathbf{\Phi}(\mathbf{p}',\mathbf{p}') + 2\partial_{\mathbf{p}}^2\partial_\lambda \mathbf{\Phi}(\mathbf{p}') + \partial_{\mathbf{p}}^2 \mathbf{\Phi}(\mathbf{p}'') + \partial_{\mathbf{p}}\partial_\lambda^2 \mathbf{\Phi})\mathbf{q}$. Solving the equations $\mathbf{\Phi}' = \mathbf{0}$ and $\mathbf{\Phi}'' = \mathbf{0}$ yields the successive derivatives of the state vector $\mathbf{p}$. Hence $\mathbf{p}' = -\partial_{\mathbf{p}}\mathbf{\Phi}^{-1}(\partial_\lambda \mathbf{\Phi})$ and $\mathbf{p}'' = -\partial_{\mathbf{p}}\mathbf{\Phi}^{-1}(\partial_{\mathbf{p}}^2 \mathbf{\Phi}(\mathbf{p}',\mathbf{p}') + 2\partial_{\mathbf{p}}\partial_\lambda \mathbf{\Phi}(\mathbf{p}') + \partial_\lambda^2 \mathbf{\Phi})$. Substituting those two expressions in equation (9b) yields the non-linear eigenvalue problem formulation.

Consider now that the system is such that we have a primary state of equilibrium defined by movements restricted to the initial plane. Use the previously introduced notation $(\cdot)_{\mathrm{I}}$ to denote a vector constrained to the primary state variable subset and $(\cdot)_{\mathrm{II}}$ to denote a vector constrained to the secondary state variable subset. Assuming a conservative system, it can be shown that the definition function vector constrained to the secondary state variable subset and evaluated at the primary path is a constant function with respect to the primary variables and the load parameter. Hence $\partial_{\mathbf{p}_{\mathrm{I}}}^k \partial_\lambda^l \mathbf{\Phi}_{\mathrm{II}} = \mathbf{0}$ for all $k \geq 0$ and $l \geq 0$. This implies, in particular, that definition function vector constrained to the secondary state itself is identically zero, and that the jacobian of the defining function is block diagonal. Hence if we rewrite equation (8) with these assumptions we get the following expressions

$$\begin{cases} \mathbf{\Phi}_{\mathrm{I}}\,|_{(\mathbf{p}_{\mathrm{I}},\lambda)} = \mathbf{0} \\ \begin{pmatrix} \partial_{\mathbf{p}_{\mathrm{I}}}\mathbf{\Phi}_{\mathrm{I}} & \mathbf{0} \\ \mathbf{0} & \partial_{\mathbf{p}_{\mathrm{II}}}\mathbf{\Phi}_{\mathrm{II}} \end{pmatrix}_{|(\mathbf{p}_{\mathrm{I}},\lambda)} \begin{pmatrix} \mathbf{q}_{\mathrm{I}} \\ \mathbf{q}_{\mathrm{II}} \end{pmatrix} = \mathbf{0} \end{cases} \tag{10}$$

As a result, the polynomial approximation, too, shows a block diagonal structure. It can be easily shown that $\mathbf{p}_{\mathrm{I}}' = -\partial_{\mathbf{p}_{\mathrm{I}}}\mathbf{\Phi}_{\mathrm{I}}^{-1}(\partial_\lambda \mathbf{\Phi}_{\mathrm{I}})$ whereas $\mathbf{p}_{\mathrm{II}}' = \mathbf{0}$. In a similar way we can find $\mathbf{p}_{\mathrm{I}}'' = -\partial_{\mathbf{p}_{\mathrm{I}}}\mathbf{\Phi}_{\mathrm{I}}^{-1}(\partial_{\mathbf{p}_{\mathrm{I}}}^2 \mathbf{\Phi}_{\mathrm{I}}(\mathbf{p}_{\mathrm{I}}',\mathbf{p}_{\mathrm{I}}') + 2\partial_{\mathbf{p}_{\mathrm{I}}}\partial_\lambda \mathbf{\Phi}_{\mathrm{I}}(\mathbf{p}_{\mathrm{I}}') + \partial_\lambda^2 \mathbf{\Phi}_{\mathrm{I}})$ while $\mathbf{p}_{\mathrm{II}}'' = \mathbf{0}$. The coefficient expressions of the criticality condition (9b) have therefore the following structure

$$(\partial_{\mathbf{p}}\mathbf{\Phi}\,\mathbf{q})' = \begin{pmatrix} (\partial_{\mathbf{p}_{\mathrm{I}}}\mathbf{\Phi}_{\mathrm{I}})' & 0 \\ 0 & (\partial_{\mathbf{p}_{\mathrm{II}}}\mathbf{\Phi}_{\mathrm{II}})' \end{pmatrix} \begin{pmatrix} \mathbf{q}_{\mathrm{I}} \\ \mathbf{q}_{\mathrm{II}} \end{pmatrix} \tag{11a}$$

$$(\partial_{\mathbf{p}}\mathbf{\Phi}\,\mathbf{q})'' = \begin{pmatrix} (\partial_{\mathbf{p}_{\mathrm{I}}}\mathbf{\Phi}_{\mathrm{I}})'' & 0 \\ 0 & (\partial_{\mathbf{p}_{\mathrm{II}}}\mathbf{\Phi}_{\mathrm{II}})'' \end{pmatrix} \begin{pmatrix} \mathbf{q}_{\mathrm{I}} \\ \mathbf{q}_{\mathrm{II}} \end{pmatrix} \tag{11b}$$

with the following expressions for the submatrix blocks

$$(\partial_{\mathbf{p}_{\mathrm{I}}}\mathbf{\Phi}_{\mathrm{I}})' = \partial_{\mathbf{p}_{\mathrm{I}}}^2 \mathbf{\Phi}_{\mathrm{I}}(\mathbf{p}_{\mathrm{I}}') + \partial_{\mathbf{p}_{\mathrm{I}}}\partial_\lambda \mathbf{\Phi}_{\mathrm{I}} \tag{12a}$$

$$(\partial_{\mathbf{p}_{\mathrm{II}}}\mathbf{\Phi}_{\mathrm{II}})' = \partial_{\mathbf{p}_{\mathrm{I}}}\partial_{\mathbf{p}_{\mathrm{II}}}\mathbf{\Phi}_{\mathrm{II}}(\mathbf{p}_{\mathrm{I}}') + \partial_{\mathbf{p}_{\mathrm{II}}}\partial_\lambda \mathbf{\Phi}_{\mathrm{II}} \tag{12b}$$

$$(\partial_{\mathbf{p}_{\mathrm{I}}}\mathbf{\Phi}_{\mathrm{I}})'' = \partial_{\mathbf{p}_{\mathrm{I}}}^3 \mathbf{\Phi}_{\mathrm{I}}(\mathbf{p}_{\mathrm{I}}',\mathbf{p}_{\mathrm{I}}') + 2\partial_{\mathbf{p}_{\mathrm{I}}}^2\partial_\lambda \mathbf{\Phi}_{\mathrm{I}}(\mathbf{p}_{\mathrm{I}}') + \partial_{\mathbf{p}_{\mathrm{I}}}^2 \mathbf{\Phi}_{\mathrm{I}}(\mathbf{p}_{\mathrm{I}}'') + \partial_{\mathbf{p}_{\mathrm{I}}}\partial_\lambda^2 \mathbf{\Phi}_{\mathrm{I}} \tag{12c}$$

$$(\partial_{\mathbf{p}_{\mathrm{II}}}\mathbf{\Phi}_{\mathrm{II}})'' = \partial_{\mathbf{p}_{\mathrm{I}}}^2\partial_{\mathbf{p}_{\mathrm{II}}}\mathbf{\Phi}_{\mathrm{II}}(\mathbf{p}_{\mathrm{I}}',\mathbf{p}_{\mathrm{I}}') + 2\partial_{\mathbf{p}_{\mathrm{I}}}\partial_{\mathbf{p}_{\mathrm{II}}}\partial_\lambda \mathbf{\Phi}_{\mathrm{II}}(\mathbf{p}_{\mathrm{I}}') + \partial_{\mathbf{p}_{\mathrm{I}}}\partial_{\mathbf{p}_{\mathrm{II}}}\mathbf{\Phi}_{\mathrm{II}}(\mathbf{p}_{\mathrm{I}}'') + \partial_{\mathbf{p}_{\mathrm{II}}}\partial_\lambda^2 \mathbf{\Phi}_{\mathrm{II}} \tag{12d}$$

One direct consequence of the block structure of the eigenvalue problem is that we can separate the examination of the eigenvalue problem in in-plane solutions and out-of-plane solutions. In the first case the determinant $\det \partial_{\mathbf{p}_\mathrm{I}} \mathbf{\Phi}_\mathrm{I} = 0$ and $\det \partial_{\mathbf{p}_\mathrm{II}} \mathbf{\Phi}_\mathrm{II} \neq 0$, while in the other case it's exactly the opposite: $\det \partial_{\mathbf{p}_\mathrm{I}} \mathbf{\Phi}_\mathrm{I} \neq 0$ and $\det \partial_{\mathbf{p}_\mathrm{II}} \mathbf{\Phi}_\mathrm{II} = 0$. Since we are primarily interested in the out-of-plane stability behavior of the system, it makes sense to concentrate the analysis on the subproblem $\partial_{\mathbf{p}_\mathrm{II}} \mathbf{\Phi}_\mathrm{II}\, \mathbf{q}_\mathrm{II}$.

Then, to make the link to what we have exposed in section 2, we may redefine the defining function restricted to the primary state as $\mathbf{\Phi}_\mathrm{I}\,|_{(\mathbf{p}_\mathrm{I},\lambda)} := \mathbf{K}_\mathrm{I}\,|_{\mathbf{p}_\mathrm{I}}\, \mathbf{p}_\mathrm{I} - \lambda\, \mathbf{e}_\mathrm{I}$ and redefine the criticality condition related to out-of-plane modes as $\partial_{\mathbf{p}_\mathrm{II}} \mathbf{\Phi}_\mathrm{II}\,|_{(\mathbf{p}_\mathrm{I},\lambda)}\, \mathbf{q}_\mathrm{II} := \mathbf{K}_\mathrm{II}\,|_{\mathbf{p}_\mathrm{I}}\, \mathbf{q}_\mathrm{II}$.

4. Analysis of some example structures

The task of setting up the specifications for the analysis is far from being obvious. Indeed, we are not facing just an engineering problem, which means it is enough that we find the critical point for a given structure. Rather, we have no precise structure at hand but only a multi-dimensional domain the structure geometry may vary within, and we are supposed to figure out what type of

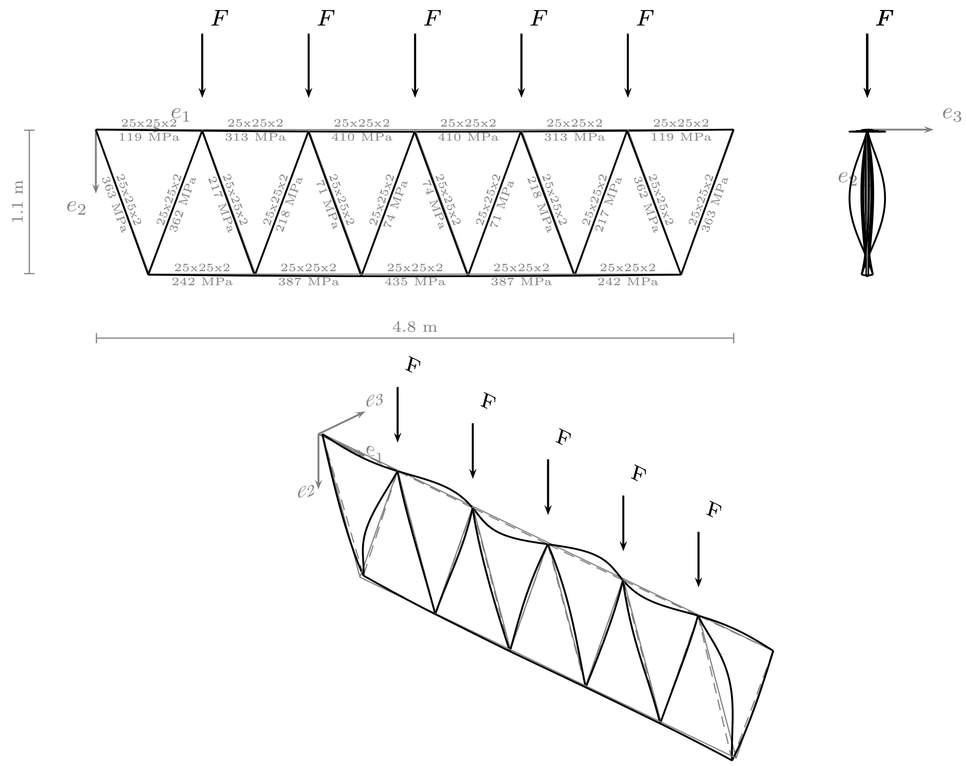

solution of linear evp:	30.8933 kN
solution of non-linear problem starting from linear evp solution:	25.1362 kN
solution of quadratic evp:	25.1248 kN
solution of non-linear problem starting from quadratic evp solution:	25.1362 kN

Fig. 3 Example truss with symmetric buckling mode

structural failure is going to happen within that domain. The investigation we are going to proceed with could therefore be referred to as some sort of pushover analysis, since we are looking for the point at which structural failure occurs.

The geometrical domain is large. It is therefore appropriate to restrict the domain to structures that are plausible from the engineering point of view. So far we have started our analysis work by investigating inverted Warren trusses with rectangular hollow section members. The reason to this is that engineers seem to favor this type of structures as structural elements of large span roofs in buildings. It is not to say that a similar type of analysis and comparison could be carried on other type of trusses as well, including types of bridge trusses and arch trusses. Once we have fixed the basic type of truss we are going to investigate, we have several geometric parameters that can vary: the number of openings in the truss, the length and the height of the truss and cross-sectional properties of each member. Cross-sectional properties can be chosen so that they are identical for all members, or alternatively cross-sectional properties are identical for top and bottom chords on one hand and for diagonals and verticals on the other. Let's examine two examples given in Figs. 3 and 4.

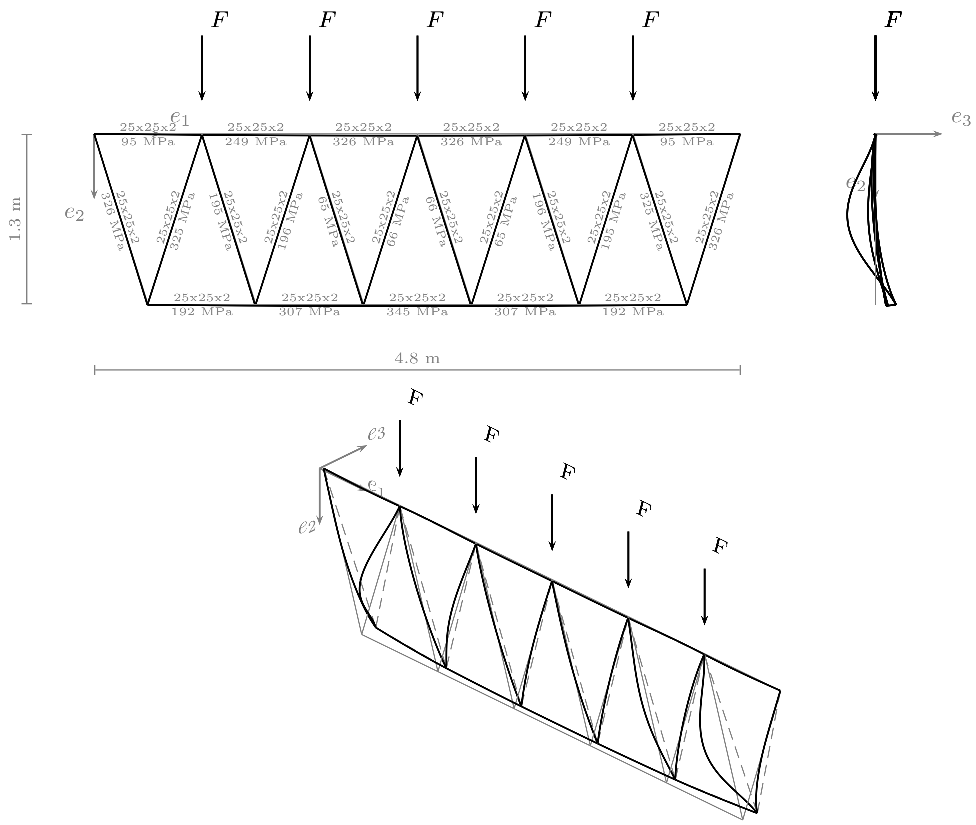

solution of linear evp:	34.6439 kN
solution of non-linear problem starting from linear evp solution:	28.6391 kN
solution of quadratic evp:	22.9412 kN
solution of non-linear problem starting from quadratic evp solution:	22.9411 kN

Fig. 4 Example truss with non-symmetric buckling mode

The key issue in these examples is the buckling mode. If the lateral movement of the upper chord of the truss is restricted at nodes, we can observe two qualitatively different buckling modes which may occur for the lowest positive buckling load. The first will be called $\mathbf{e}_2$-symmetric (shortly just symmetric) due to the fact that the projection of the buckling mode on the plane perpendicular to the axis of the beam is a symmetric curve. It is characterized by lateral sinusoidal displacement of the upper chord such that nodal points are not moving in lateral direction and usually small lateral displacement of the lower chord. An example of symmetric buckling mode is given in Fig. 3.

The second buckling mode will be called non-symmetric due to the fact that the projection on the perpendicular plane forms a non-symmetric curve. It is characterized by relatively large lateral displacement of the lower chord together with buckling of the compressed diagonals. The upper chord undergoes torsion, but lateral displacement does not occur altogether. It can be remarked that in addition to memberwise buckling of a given diagonal, there is some rigid body motion characterized by lateral sway of the lower end of the diagonal. An example of non-symmetric buckling mode is given in Figure 4. As we can notice, in the symmetric mode example (Fig. 3) the non-linear system solution converges to the same point, whether we start from the linear or the quadratic eigenvalue problem solution. On the other hand in the non-symmetric mode example (Fig. 4) the non-linear system solution does not converge to the same point, depending whether we start from the linear or the quadratic eigenvalue problem solution.

Consider the “reference solution” to be the solution given by the Newton algorithm, where we used the solution of the *quadratic* approximation as an initial guess. The reference solution corresponds therefore to the true solution of the non-linear problem. On the other hand, let's call “candidate solution” the solution given by the Newton algorithm, where we used the solution of the *linear* approximation as an initial guess. If everything goes well, the candidate and reference solutions should match, as it is the case in Fig. 3. However, the example in Fig. 4 shows that sometimes the candidate solution does not match the reference solution.

In the following interaction diagrams (Figs. 5-8), we shall plot, for some parameter values of the truss, the boolean function whether or not the candidate solution matches the reference one. The total truss length is on the abscissa of the diagram, the truss height on the ordinate. We have divided the diagram in two domains: domain $\mathcal{D}_{\text{lin}}$, where the candidate and reference solution match, and domain $\mathcal{D}_{\text{qua}}$, where the candidate and reference solutions do not match. We can also state that the boundary that separates the domains $\mathcal{D}_{\text{lin}}$ and $\mathcal{D}_{\text{qua}}$ from each other is nearly linear in the case of small cross-sections. The diagrams have been drawn so that the display area is meaningful from the engineering point of view, and hence what happens outside the display area has not been investigated. As a general statement, we can claim that non-symmetric buckling mode and failure of the linearized eigenvalue problem to provide a good initial guess point for non-linear system solver occur for rather high trusses. The average slope of boundary separation line is around $L/h \approx 4.0$. Obviously this type of truss geometry is not quite a usual design.

If we investigate trusses made of larger cross-sections, as in our example (Fig. 8) we have 120×120×6 square hollow sections for all members, the pattern changes quite radically. First remark can be said about the buckling mode. In the case of large cross-sections the switch from symmetric mode to non-symmetric mode does not follow at all the boundary line between $\mathcal{D}_{\text{lin}}$ and $\mathcal{D}_{\text{qua}}$. In Fig. 8 non-symmetric mode is found high above the display area, which means that linearized eigenvalue problem may fail to give a good starting point for non-linear system solver even if the buckling mode is symmetric. The second remark can be given on the shape of the boundary between the domains $\mathscr{D}_{\text{lin}}$ and $\mathscr{D}_{\text{qua}}$, which is definitely not linear. Once the total length of the truss is larger than a given number around 51.5m, no matter how high the truss, we will need to use the quadratic eigenvalue solution as a starting point to the non-linear solver.

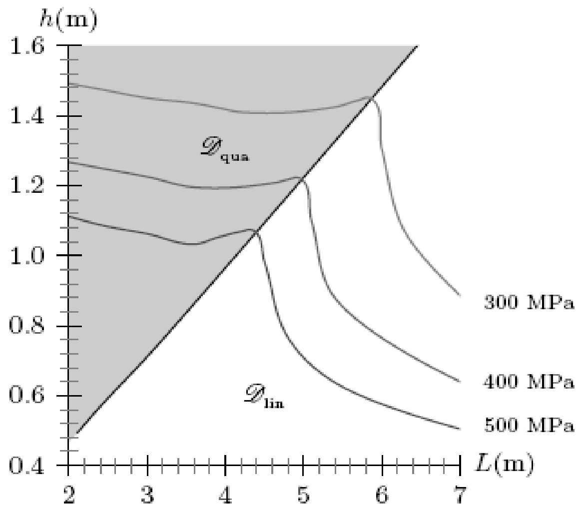

Fig. 5 Interaction diagram for a Warren truss with 12 diagonals, total length *L*, total height *h*, all members 25×25×2 square hollow sections.

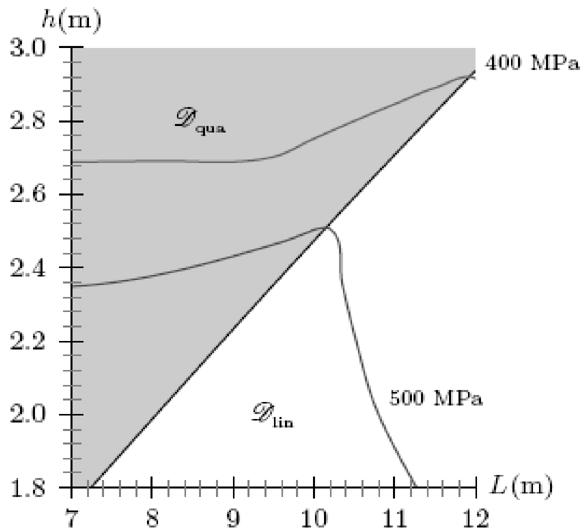

Fig. 6 Interaction diagram for a Warren truss with 12 diagonals, total length *L*, total height *h*, all members 50×50×4 square hollow sections.

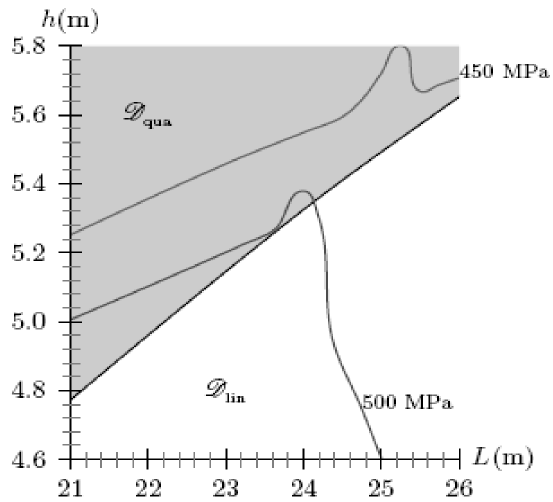

Fig. 7 Interaction diagram for a Warren truss with 12 diagonals, total length *L*, total height *h*, all members 80x80x5 square hollow sections

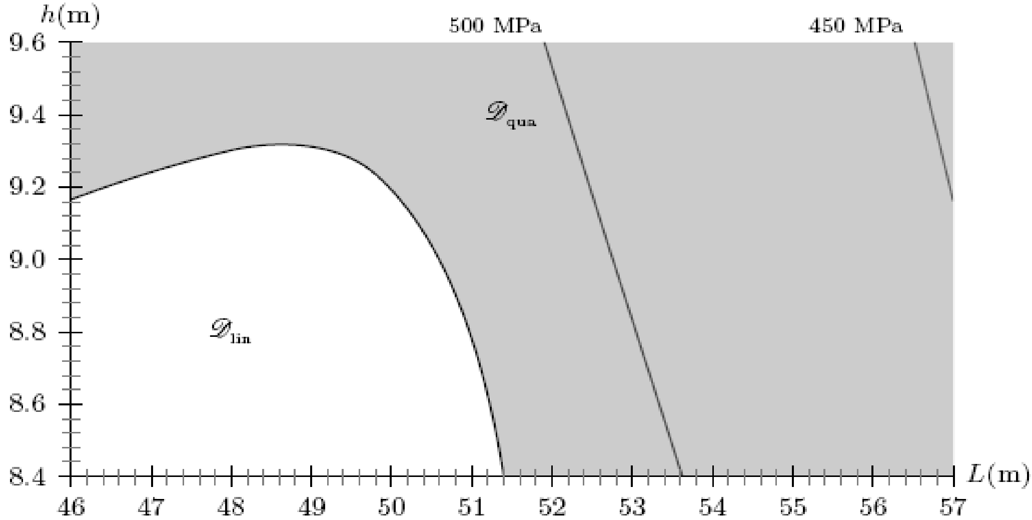

Fig. 8 Interaction diagram for a Warren truss with 12 diagonals, total length *L*, total height *h*, all members 120×120×6 square hollow sections

5. Conclusions

A number of Warren trusses have been investigated for various stability related properties. The main property that is of practical interest is whether a designer can rely on the linearized eigenvalue problem solution as an approximation to a non-linear problem. It turns out that if the primary path of a given system is highly non-linear, the solution of linearized eigenvalue problem not only gives a bad approximation, but it also fails to be within the radius of convergence of the minimum positive eigenvalue of the non-linear system, assuming that we apply an iterative solver to correct the initial guess given by the linearized eigenvalue problem. In most cases this drawback can be fixed if we use the solution of a quadratic eigenvalue problem as a staring point for the iterative solver. Since we assumed that the lateral displacement of the upper chord is restricted at nodal points, the trusses that have been investigated are all highly non-linear and therefore they give good examples of structures that are problematic to analyze using linearized eigenvalue solver.

All the trusses that have been investigated are composed of steel rectangular hollow cross-sections. This type of trusses is widely used in construction, and therefore it is natural to verify the behavior of stability related numeric methods with this type of structures first. Fortunately, it seems that the geometries of most engineering applications are such that even linearized eigenvalue problem solution gives at least a good starting point for non-linear solver. However, the situation with open thin-walled steel cross-sections or wood cross-sections is far from being safe. This is due to the low torsional rigidity of these types of cross-sections, in contrast to closed cross-sections. Therefore a wider range of truss geometries using a wider range of cross-sections should be investigated in order to complete the picture.

References

Attard, M. (1990), "General non-dimensional equation for lateral buckling", *Thin-Walled Structures*, **9**(1-4), *Special Volume on Thin-Walled Structures: Developments in Theory and Practice*, 417-435.

Battini, J.M., Pacoste, C. and Eriksson, A. (2003), "Improved minimal augmentation procedure for direct computation of critical points", *Computer Methods in Applied Mechanics and Engineering*, **192**(16-18), 2169-2185.

Chan, S.L. and Cho, S.H. (2008), "Second-order analysis and design of angle trusses Part I: elastic analysis and design", *Engineering Structures*, **30**(3), 616-625.

Golubitsky, M. and Schaeffer, D. (1985), "Singularities and Groups in Bifurcation Theory", *Applied Mathematical Sciences*, **17,** Springer Verlag.

Hancock, G., Davids, A., Key, P., Lau, S. and Rasmussen, K. (1990), "Recent developments in the buckling and nonlinear analysis of thin-walled structural members", *Thin-Walled Structures*, **9(**1-4), *Special Volume on Thin-Walled Structures: Developments in Theory and Practice*, 309-338.

Iwicki, P. (2010), "Sensitivity analysis of critical forces of trusses with side bracing", *Journal of Constructional Steel Research*, **66**(7), 923-930.

Govaerts, W. (2000), "Numerical methods for bifurcations of dynamical equilibria", *Society for Industrial and Applied Mathematics*, Philadelphia.

Keener, J. and Keller, H. (1973), "Perturbed bifurcation theory", *Archive for Rational Mechanics and Analysis*, **50**, 159-175.

Koiter, W.T. (1945), "Over de stabiliteit van het elastisch evenwicht", PhD Thesis, Technische Hogeschool, Delft, English tranlations: NASA TT F10, 833 (1967) and AFFDL, TR-7025 (1970).

Lopez, S. (2002), "Detection of bifurcation points along a curve traced by continuation method", *International Journal for Numerical Methods in Engineering*, **53**, 983-1004.

Masur, E.F. and Cukurs, A. (1956), *Lateral Buckling of Plane Frameworks*, Engineering Research Institute, The University of Michigan Ann Arbor, Project 2480.

Moore, G. and Spence, A. (1980), "The calculation of turning points of non-linear equations", *SIAM Journal of Num. Analysis*, **17**, 567-576.

Mäkinen, J., Kouhia, R., Fedoroff, A. and Marjamäki, H. (2012), "Direct computation of critical equilibrium

states for spatial beams and frames", *International Journal for Numerical Methods in Engineering*, **89**(2), 135-153.
Rheinboldt, W.C. (1986), *Numerical Analysis of Parametrized Nonlinear Equations*, Wiley.
Riks, E. (1974), "The incremental solution of some basic problems in elastic stability", Technical Report NLR TR 74005 U, National Aerospace Laboratory, The Netherlands.
Schardt, R. (1966), "Eine erweiterung der technische biegetheorie zur berechnung prismatischer faltwerke", *Stahlbau*, **35**, 161-171.
Seydel, R. (1979), "Numerical calculation of branch points in nonlinear equations", *Numer. Math.*, **33**, 339-352.
Sridharan, S. and Rafael, B. (1985), "Interactive buckling analysis with finite strips", *International Journal for Numerical Methods in Engineering*, **21**, John Wiley and Sons, Ltd.
Trahair, N. and Vacharajittiphan, P. (1975), "Analysis of Lateral Buckling in Plane Frames", *Journal of the Structural Division*, **101(7)**, 1497-1516.
Trahair, N. and Chan, S.L. (2003), "Out-of-plane advanced analysis of steel structures", *Engineering Structures*, **25**, 1627-1637**.**
Trahair, N. (2009), "Buckling analysis design of steel frames", *Journal of Constructional Steel Research*, **65**, 1459-1463.
Vlasov, V.Z. (1961), *Thin-walled Elastic Beams*, National Science Foundation and Department of Commerce.
Vrcelj, Z. and Bradford, M.A. (2006), "Elastic distortional buckling of continuously restraine I-section beam-columns", *Journal of Constructional Steel Research*, **62**, 223-230.
Wriggers, P. and Simo, J.C. (1990), "A general procedure for the direct computation of turning and bifurcation problems", *Computer Methods in Applied Mechanics and Engineering*, **30**, 155-176.